MJSAT

Malaysian Journal of Science and Advanced Technology

journal homepage: https://mjsat.com.my/

In-silico Assessment of Radiation Shielding Effectiveness of Some Materials used in Interior Building Decorations

Paul S. Ayanlola*[1], Mustapha K. Lawal[2] Omololu I. Agbelusi[3] and Gbadebo A. Isola[1]

[1]*Department of Pure and Applied Physics, Ladoke Akintola University of Technology, Ogbomoso, Nigeria.*
[2]*Department of Science Laboratory Technology, Ladoke Akintola University of Technology, Ogbomoso, Nigeria.*
[3]*Department of Physical Sciences, Chrisland University, Agbeokuta, Nigeria.*

KEYWORDS

Building materials
Interior decorations
Radiation shielding
Radiation safety

ARTICLE HISTORY

Received 29 January 2025
Received in revised form 28 February 2025
Accepted 15 May 2025
Available online 18 June 2025

ABSTRACT

The increasing trend in the use of decorative building materials for aesthetically pleasing purposes while neglecting the shielding effectiveness of these materials against penetrative radiation is a cause of concern radiologically. It is in view of this, that the present study investigates the radiation shielding properties of concrete, gypsum, glass and ceramic tile in order to intimate the end users of the radiological safety of these materials as regard interior building decorations. The linear- and mass-attenuation coefficient (LAC, MAC), half- and tenth-value layers (HVL, TVL), mean free path (MFP), effective atomic number (Z_{eff}), and electron density (N_{eff}) of the selected building materials were calculated for photon energies in the range between 0.05 to 1.408 MeV. The peak MAC value was observed at low energies for all materials, while the lowest values were found at high energies. Furthermore, as the thickness increases, the materials' capacity to attenuate high-energy photons also increases. These findings of the study encourage the continuous use of ceramic tiles in building flooring compared to concrete flooring, as ceramic tiles proofed to be sufficient in attenuating photons more than concrete. The usage of gypsum as building ceilings, concrete as walls and glass as windows are justified also to attenuate the particulate radiations. Thus, while concerted effort are being made towards achieving atheistically pleasing interior building decorations, the end users are hereby safe radiologically as these materials are effective in shielding against radiation even at low energy.

1. INTRODUCTION

Buildings are enclosed structures featuring roofs and walls that typically remain fixed in one location, such as homes or factories [1]. These structures vary in numerous sizes, shapes, and purposes, having been modified throughout human history for a wide range of functions. Buildings fulfil multiple societal needs, mainly providing shelter, security, living areas, privacy, storage for possessions, and spaces for comfortable living and working. As a form of shelter, a building creates a physical division between the human living environment (a place of comfort and safety) and the outside world (which can at times be harsh and dangerous). Buildings may be adorned both inside and out to enhance their aesthetic appeal and improve their functional usability for those who occupy them [2]. However, a building can become contaminated due to the materials that comprise its structure [3].

Radiologically, naturally occurring radioactive materials (NORMs) such as ^{238}U, ^{232}Th, and ^{40}K are found in trace amounts in construction materials, including decorative stone, bricks, and some additives used in concrete [3 - 5]. Due to this, there is a growing focus on utilizing materials that are less radioactive for interior design purposes. Nonetheless, the presence of these radionuclides in environmental contexts is influenced by the geochemical makeup of the surrounding environment, which raises concerns. This is because ionizing radiation (IR) has enough energy to dislodge electrons from atoms, altering the chemical structure of the materials with which it comes into contact. In living tissues, this alteration can lead to damaging effects on DNA, potentially resulting in cell

*Corresponding author:
E-mail address: Paul S. Ayanlola < psayanlola28@lautech.edu.ng >.
https://doi.org/10.56532/mjsat.v5i2.474

death or mutations, such as cancer [6,7]. Therefore, uncontrolled ionizing radiation poses significant risks and can be fatal.

While buildings serve as a fundamental source of shelter, the materials utilized in construction should effectively guard against penetrating radiation, such as photons that might originate from the ground beneath the structure or from external radiation sources. The main objective of radiation shielding is therefore to minimize exposure to these penetrative radiations. Consequently, appropriate measures for radiation protection are consistently required for a secure living environment and public health. The United States Nuclear Regulatory Commission (NRC) describes radiation shielding as the process of decreasing radiation by placing an absorbing material barrier between a radioactive source and an individual, work area, or radiation-sensitive equipment. Shielding is essential for both directly ionizing and indirectly ionizing radiation [8]. The materials selected for shielding are contingent upon the type of radiation involved; therefore, while certain radiation shielding materials are effective against specific radiation types, they might not provide protection against others. Furthermore, choosing the appropriate material can result in space savings, reduced material usage, and enhanced safety for occupants.

Metals with moderate to high atomic numbers (Z), such as steel, iron, and lead, are recognized as some of the most efficient materials for IR shielding. However, these materials are generally not used in construction due to issues related to durability, cost, and environmental safety. As a result, medium-mass materials like bricks, sand, cement, and concrete are commonly utilized as foundational media in construction and for general shielding applications [9,10]. Additionally, various metamorphic rocks, crystalline, and ceramic materials such as marble, glass, and tiles are also utilized in building construction and for aesthetic purposes [3,11,12]. Building materials including soil, rocks, aggregates, concrete, bricks, steel, and polymers have been extensively studied regarding their protective capabilities against natural disasters and their durability. In this context, the radiation shielding characteristics of materials used in residential and non-residential buildings have garnered significant interest [9,10,13,14].

In this study, decorative materials including concrete, gypsum, glass, and ceramic tiles were examined to assess their effectiveness in protecting against penetrating gamma rays. Concrete is a widely used material in both building construction and decoration. It is composed of a mixture of cement, fine aggregate, coarse aggregates, and water, which solidifies over time [4]. This material offers various benefits, such as its availability, cost efficiency, and simplicity of construction [15]. As a composite material made up of cement, aggregates (like sand and gravel), and water, concrete can be shaped into different forms and sizes. Research has shown that concrete effectively attenuates IR due to its high density and composition, which enhances the absorption and scattering of radiation particles [16,17].

Gypsum, also known as Plaster of Paris, has been utilized as a construction material for hundreds of years and can be found naturally in sedimentary formations from ancient ocean floors [5]. The application of gypsum in plasterboard for interior design in contemporary structures has been increasing due to the rapid development of infrastructure by individuals, private enterprises, and government entities at various levels. This trend is largely because the final output of such designs enhances the appearance of buildings, making them visually appealing. Additionally, due to advancements in technology, the use of gypsum plasterboard for indoor decorations is surpassing traditional methods of interior design.

In construction, tiles are usually thin sheets employed for enhancing both the interior and exterior aesthetics of buildings, providing several beneficial features. The tile sector has been largely dominated by porcelain and ceramic tiles. Materials for ceramic tiles, including earthenware and stoneware, are often insufficiently durable for outdoor applications as they tend to absorb significant amounts of water [18]. Conversely, porcelain tiles are created from a clay that has a paste-like consistency and is baked at elevated temperatures. Porcelain tiles are extremely resistant to water and are regarded as more durable and more suitable for extensive applications compared to other ceramic tiles [19].

The incorporation of glass in architectural design has gained significant traction in recent years due to its exceptional advantages. Nowadays, architects and designers favour glass as their primary material, not only for its visual appeal but also for its reliable performance. Glass uniquely integrates the exterior and interior spaces, effectively connecting the outdoors with the indoors. Compared to other construction materials, glass excels in aesthetics by enhancing a building's design with vibrant colors and distinct character. Therefore, utilizing glass as a decorative element can lower energy expenses, boost property value, and enhance the comfort of occupants [20].

Conventional radiation shielding materials such as lead, borated polyethylene, and steel have been extensively researched due to their well-known and effective characteristics, commonly utilized in high-radiation settings like nuclear reactors, hospitals, industries, and space exploration. However, there has been less focus on alternative materials like concrete, gypsum, glass, and ceramic tiles, as they were not originally intended for radiation shielding. Additionally, these materials are frequently employed in situations where radiation protection is not the primary consideration. Consequently, while radiation shielding in construction is crucial, it has not garnered as much interest. Moreover, these materials are primarily chosen for their structural integrity and visual appeal rather than their radiation shielding capabilities. Therefore, detailed radiation studies on these materials may not be prioritized, particularly when they are not viewed as a main shielding barrier against radiation.

Hence, while individuals have the freedom to choose from the materials mentioned for building design, it is important to consider their ability to protect against radiation, whether it originates from natural sources or human activities. Moreover, a personal preference for visually appealing interior design should not compromise indoor air quality. Consequently, the properties of building materials must meet acceptable standards to ensure safe living conditions. Therefore, it is essential to explore the radiation shielding effectiveness of these materials to inform users about their radiological safety in relation to interior building designs and radiation safety. Conducting a radiological impact assessment of building materials to evaluate and manage the radiological effects on both the public and the environment is a crucial and sensitive task, particularly in light of the principles of sustainable development goals of the United Nations.

The assessment of radiation shielding characteristics for materials such as concrete, gypsum, glass, and ceramic tiles across various energy levels necessitates the collection of extensive data. In this context, performing manual calculations is quite labor-intensive, and there are instances where errors can occur during these calculations. Research has shown that theoretical computer-based tools like WinXCOM, GEANT4, FLUKA, and other numerous Monte Carlo simulations for examining radiation transport and interactions are favored by scientists to eliminate errors, decrease calculation time, and lessen the need for consumables during the experimental stage. Nevertheless, these software programs are limited to calculating just one specific parameter, the mass attenuation coefficient (MAC), among several pertinent radiation shielding characteristics. Hence, this study employs Phy-X/PSD.

2. SHIELDING PROPERTIES AND DEFINITION

The qualities of an effective shielding material include its density and atomic number, linear- and mass-attenuation coefficient, half-value layer and tenth-value layer, mean free path, exposure buildup factor, and effective atomic number, all of which need to be analysed to assess the appropriateness of the suggested materials for radiation shielding applications.

2.1 Density and Atomic Number

The efficacy of a radiation shielding substance is primarily influenced by its atomic number and density. Density (ρ) represents the mass (M) of a material relative to its volume (V). It is widely recognized that an increase in a material's density enhances the likelihood of interaction between an incoming photon and the absorbing medium [21].

2.2 Linear and Mass Attenuation Coefficients

The need for shielding materials stems from the concept of attenuation. Attenuation refers to the extent to which a wave or ray's impact can be diminished through the use of shielding materials. The calculations and characteristics related to radiation shielding for any material are expressed in terms of the linear attenuation coefficient (LAC). The LAC is a measurement that indicates how readily photons can penetrate a material. It plays a pivotal role in assessing the influence of gamma radiation of a specific energy on a material. The attenuation coefficient is utilized to estimate the transmission of gamma radiation through a specific thickness of shielding material or to determine the necessary thickness of shielding material to achieve a desired level of attenuation. When interacting with the target material, the incoming photon will not scatter but will either be absorbed by the shielding material or pass through it, ultimately reaching the detector. As photons engage with the target material, their intensity diminishes due to photon interactions like the photoelectric effect, Compton scattering, or pair production. Therefore, the LAC represents the cumulative probabilities of these three photon interaction processes [21-24]. The attenuation of a mono-energetic narrow gamma photon beam adheres to the Beer-Lambert law, which is represented by equations (1) and (2).

$$I(cm^{-1}) = I_O e^{-\mu t} \tag{1}$$

which implies that,

$$\mu(cm^{-1}) = \frac{1}{t}\ln\left(\frac{I_O}{I}\right) \tag{2}$$

In the equation, I represent the initial intensity of photons, while I_0 denotes the intensity of the photons after they have been attenuated; t indicates the thickness of the absorbing material, and μ refers to the linear attenuation coefficient (LAC). The attenuation coefficients for gamma rays depend inversely on the energy of the gamma rays and are directly related to the atomic number of the elements that make up the shielding material.

Furthermore, if the absorbing substance consists of compounds or a uniform mixture, the mass attenuation coefficient μ_m (MAC) can be estimated using equation (3) as a weighted total of the coefficients of its individual elements [22-24].

$$\mu_m(cm^2/g) = \left(\frac{\mu}{\rho}\right) = \sum_{i=1}^{n} w_i \left(\frac{\mu}{\rho}\right)_i \tag{3}$$

where, ω_i is weight fraction, $\left(\frac{\mu}{\rho}\right)_i$ is MAC of the i^{th} constituent element. This calculation facilitates the assessment of the effectiveness of materials in shielding against gamma radiation by considering both the linear attenuation coefficient and the density of the material. For a specific chemical compound, the weight fraction is calculated using equation (4)

$$w_i = \frac{n_i A_i}{\sum_i n_i A_i} \tag{4}$$

where A_i is the atomic weight of i^{th} element and n_i is the number of formula units in the compound.

2.3 Half- and Tenth-Value Layers

The half-value layer (HVL) and tenth-value layer (TVL) are crucial factors in the creation of efficient radiation shielding materials. These values indicate the thickness of the material required to diminish the incoming radiation on the substance by 50% and 10%, respectively, after it has passed through a protective shield [23-26]. The HVL and TVL can be calculated using the equations (5) and (6) respectively

$$HVL = \frac{\ln(2)}{\mu} \tag{5}$$

$$TVL = \frac{\ln(10)}{\mu} \tag{6}$$

2.4 Mean Free Path

The mean-free path (MFP), expressed by equation (7) refers to the average distance a photon travels before undergoing two consecutive interactions. It characterizes the thickness of the shielding material that reduces the initial radiation intensity to 36.8% [23,27-29].

$$MFP = \frac{1}{\mu} \tag{7}$$

2.5 Effective Atomic Number and Electron Density

Another factor related to radiation interaction that is used to describe the attenuation characteristics of mixtures or

compounds in relation to pure elements is the effective atomic number (Z_{eff}). This is defined as the atomic number that represents a mixture or compound and interacts with photons in a manner equivalent to a single elemental substance. Z_{eff} varies with energy, is similar to the atomic numbers of elements, and characterizes the composition of the material based on comparable elements [23,27]. It is computed using equation (8).

$$Z_{eff} = \frac{\sum_i w_i A_i \left(\frac{\mu}{\rho}\right)_i}{\sum_i w_i \frac{A_i}{Z_i} \left(\frac{\mu}{\rho}\right)_i} \tag{8}$$

The effective electron density (N_{eff}) is defined as the quantity of electrons present per unit mass of a material. It serves to describe how photons interact with matter in the context of radiation protection, assess the capability of a material to shield against radiation, and develop more effective shielding substances to reduce radiation exposure. N_{eff} depends on Z_{eff} and can be computed using equation (9).

$$N_{eff} = \frac{N_A Z_{eff}}{< A >} \tag{9}$$

where <A> and N_A are the mean atomic mass of the sample and Avogadro's constant respectively.

2.6 Buildup Factor

Buildup factor is a correction factor used to account for the increased radiation transmission observed through shielding materials due to scattered radiation. It serves as the main component in the formulation of radiation shielding materials. Buildup factors are influenced by the energy of the primary radiation, the type of shielding material, and its thickness. Numerous methods have been documented for calculating buildup factors; however, the calculation of energy absorption and exposure buildup factors (EABF and EBF) using equivalent atomic number and geometric fitting methods is commonly employed.

The equivalent atomic number (Z_{eq}) plays a crucial role in comprehending radiation shielding design. It is a parameter that depends on energy, representing the characteristics of a shielding material through the lens of equivalent elements. This value needs to be within a defined energy range, between the atomic numbers Z_1 and Z_2 (where $Z_1 < Z_2$), and it is derived using equation (10).

$$Z_{eq} = \frac{Z_1(\log R_2 - \log R) + Z_2(\log R - \log R_1)}{\log R_2 - \log R_1} \tag{10}$$

where R_1 and R_2 are the $\frac{\mu_{Comp}}{\mu_{Total}}$ ratios corresponding to the elements with atomic numbers Z_1 and Z_2, respectively, and R is the $\frac{\mu_{Comp}}{\mu_{Total}}$ ratio for the proposed shielding material at a specific energy, which lies between the ratios R_1 and R_2.

To achieve a more precise outcome for the buildup factor, Z_{eq} values for the materials, along with the interpolated GP-fitting parameters (b, c, a, X_K, d), were determined utilizing the interpolation formula outlined in the equation. (11)

$$C = \frac{C_1\left(\log Z_2 - \log Z_{eq}\right) + C_2\left(\log Z_{eq} - \log Z_1\right)}{\log Z_2 - \log Z_1} \tag{11}$$

where C_1 and C_2 represent the parameters for GP fitting, which are typically derived from the ANSI/ANS-6.4.3 standard database covering energy levels from 0.015 to 15 MeV, up to a penetration depth of 40 MFP [23,24,30]. This corresponds to Z_1 and Z_2, between which the equivalent atomic number (Z_{eq}) of the proposed shielding materials falls. This calculation is crucial for acquiring accurate insights into the behaviour and properties of materials across various energy ranges.

The EABF and EBF for the materials is then calculated using the obtained fittings parameters expressed by equations (12) and (13).

$$B(E,x) = \begin{cases} 1 + (b-1)\dfrac{(K^x - 1)}{(K-1)} & for\ K \neq 1 \\ 1 + (b-1)x & for\ K = 1 \end{cases} \tag{12}$$

where,

$$K(E,x) = cx^a + d\frac{\tanh\left(\frac{x}{X_K} - 2\right) - \tanh(-2)}{1 - \tanh(-2)}x \quad \leq 40\ MF \tag{13}$$

where x is the penetration depth in MFP, E is the energy of the incident photon, K is the photon dose multiplicative factor and represent the spectrum shape change, and (b, c, a, X_k, d) are the calculated GP fitting parameters in the previous step. The procedures for calculating EABF and EBF are identical, differing only in the coefficients applied.

3. METHODOLOGY

The radiation shielding parameters namely MAC, LAC, HVL, TVL, MFP, Z_{eff}, N_{eff}, and Z_{eq} of each material was calculated using the Phy-X/PSD (Figure 1a), a software developed for the calculation of parameters relevant to radiation shielding and dosimetry [31]. Although, several software such as WinXCOM [32,33], early developed as XCOM [34] and XMuDat [35], ZXCOM [36], and BXCOM [37] have been developed for calculation of MACs for elements, compounds and mixtures in the continuous energy region, and for the calculation of EBF and EABF parameters for the compounds and mixture. However, Phy-X/PSD was chosen because of its versatility in estimating all the aforementioned shielding parameters simultaneously in a wide energy range. In addition, the software eliminates the manual calculations of all these radiation shielding parameters in a fast way and also increase the accuracy of the result for infinite number of different materials [30]. The software has been validated by comparing it results with both experimental data and those available in literature and found to agree very well [38, 39].

The calculation of the radiation shielding parameters defined by Equation 1 to 13 in the software involves three major steps of material definition, selection of energies; and the shielding parameters of interest. The material definition is the first step and it involves the declaration and entering of the composition and density (g/cm^3) of the material under investigation. In this study, the material composition was defined as weight fraction, the sum of which equals 1 for each material. The properties of the building materials considered in this study are listed in Table 1. The constituent weight fraction of each material was extracted from NIST XCOM database [33]. For the energy selection, two energy regions, 15 keV - 15

MeV and 1 keV - 100 GeV, as well as some well-known radioactive sources (^{22}Na, ^{55}Fe, ^{60}Co, ^{109}Cd, ^{131}I, ^{133}Ba, ^{137}Cs, ^{152}Eu and ^{241}Am) along with their energies and some characteristic X-ray energies obtained through secondary sources have been predefined in the software and are available for selection and usage. For this study, radioactive sources of ^{241}Am, ^{152}Eu, ^{137}Cs, and ^{60}Co were selected covering photon energies in the range between 0.059 to 1.408 MeV, capturing both low and high energy photons effectively. This energy range encompasses the most common radiation sources present naturally in the environment and those used in medical, industrial and nuclear applications [6,7]. Thereafter, the radiation shielding parameters defined by Equations 1 to 13 and already encoded in the software were selected and analysed. The results were output in a well-designed MS excel file. The entire process followed a sequential and logical pattern describe by the flow chart in Figure 1b.

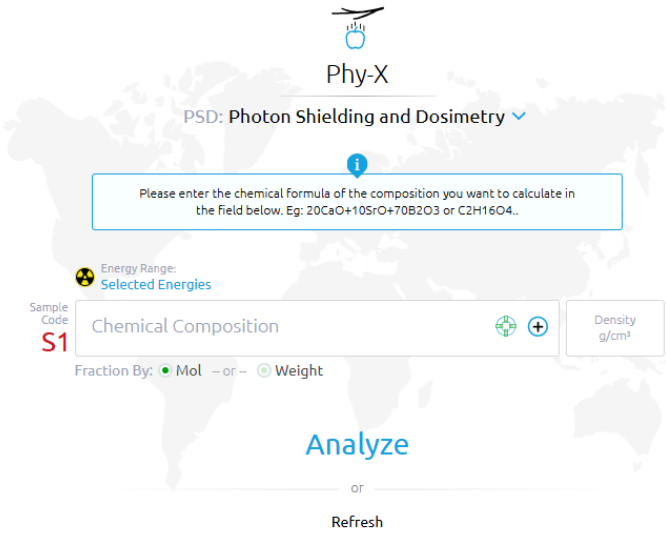

Fig. 1a. Interface of the Phy-X/PSD software.

Table 1. Building materials considered in this study [34]

Material	Code	Density (g/cm^3)	Fraction by weight
Concrete (Portland)	M1	2.30	0.01H + 0.001C + 0.529107O + 0.016Na + 0.002Mg + 0.033872Al + 0.337021Si + 0.013K + 0.044Ca + 0.014Fe
Gypsum	M2	2.32	0.023416H + 0.557572O + 0.186215S + 0.232797Ca
Glass	M3	2.23	0.040064B + 0.539562O + 0.028191Na + 0.011644Al + 0.37722Si + 0.003321K
Ceramic Tiles	M4	2.30	0.485724O + 0.013093Mg + 0.084885Al + 0.321175Si + 0.018819K + 0.031566Ca + 0.044738Fe

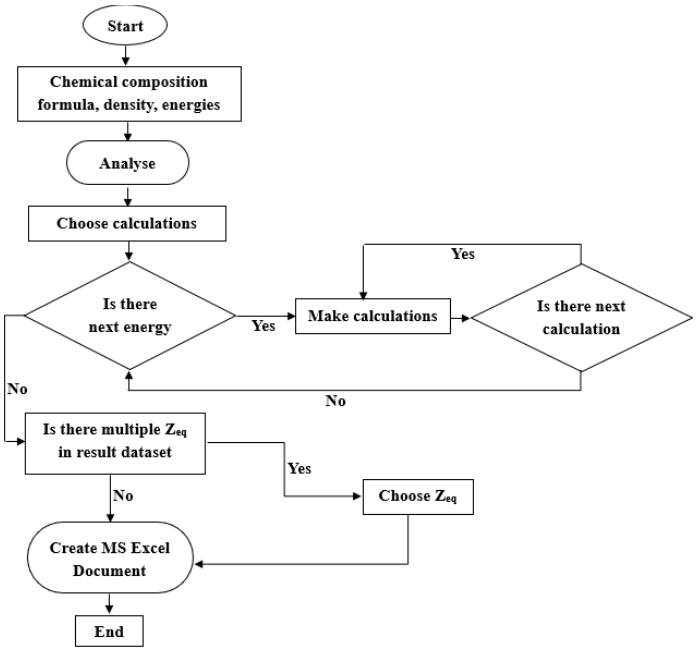

Fig. 1b. Procedure followed in estimating the shielding parameters.

4. Results and Discussion

Presented in Figure 2 are the result obtained for the MAC and LAC values of the investigated materials. The MAC values for the interaction of photons with each building material examined are illustrated in Figure 2a, with respect to the photon energy range of 0.059 – 1.408 MeV. This figure indicates that M2 (gypsum) exhibits the highest MAC value at lower energies and remains slightly higher than other materials at elevated energies. A high MAC is typical observed at lower photon energies because the probability of interactions such as photoelectric effect which dominant at low energies significantly increases, leading to greater absorption of radiation within the material. In addition, materials containing elements of higher atomic number generally exhibit higher attenuation at lower energies. Thus, the presence of S and Ca in gypsum (M2) at high weight fraction compare to the presence of Ca and Fe in ceramic tiles (M4) and concrete (M1) at low weight fractions influenced the value of MAC of these materials at lower energies. This shows that M2 is more suitable in shielding against radiation at low energy compare to M1, M3 and M4. Overall, the peak MAC value was observed at low energies for all materials, while the lowest values were found at high energies. This attribute enhances the applications of these materials in interior building decorations where radiation shielding is not the primary concern, as no radiation is too low to cause biological damage.

Furthermore, Figure 2b clearly shows that as the photon energy rises, the LAC value experiences a steep decline. This decreasing trend aligns with the prevailing photoelectric absorption mechanism at 59 keV and Compton scattering at 661, 1173, and 1332 keV [19,40]. At lower photon energies, the attenuation values follow the path of photoelectric absorption, inversely related to E^3. At intermediary energy levels, Compton scattering takes precedence in the attenuation process, with attenuation inversely related to E. Additionally, attenuation values remain stable for energies at or exceeding 1.022 MeV,

since the pair production process is the dominant factor in this region. It is evident that the ability of the sample to attenuate relates to its composition, indicating that gamma photons result in greater attenuation as the sample quantity increases [41]. In general, the attenuation coefficient at lower energies is approximately three times greater than that at higher photon energies.

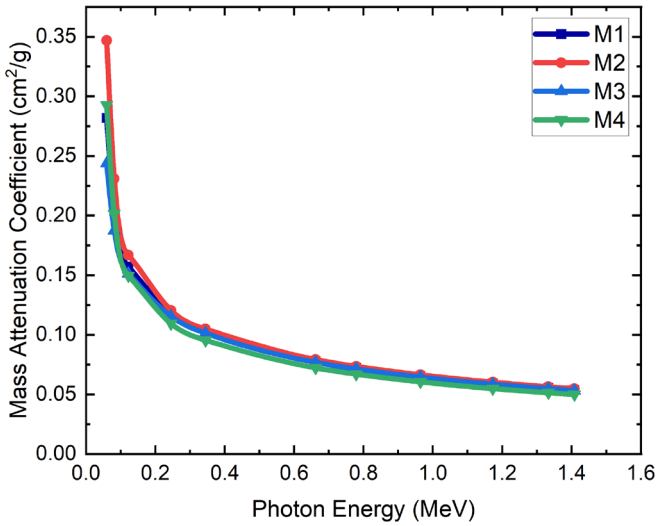

(a)

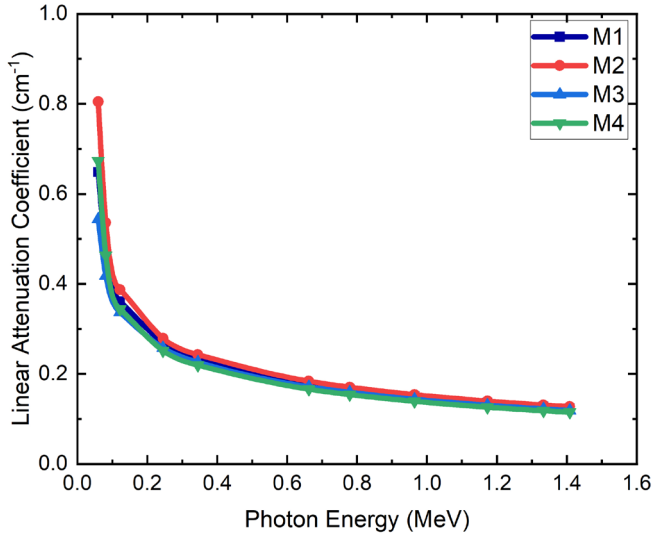

(b)

Fig. 2. (a) Mass- (b) Linear-attenuation coefficients of the building materials as a function of photon energy.

The variation of half-value layers (HVL) and tenth-value layers (TVL) in relation to photon energy is shown in Figures 3a and b, respectively. Figure 3a indicates that M4 (ceramic tile) has the highest HVL values, ranging from 1 to 6 cm, whereas M2 (gypsum) exhibits the lowest HVL, with values between 0.8 and 5.5 cm. These findings suggest that materials with greater density result in a lower HVL, which improves the material's shielding efficacy [18,19,23,24,41]. Moreover, the results indicate that the building materials under consideration display the lowest HVL at the minimal photon energy level. This corresponds to the outcomes obtained for the TVL of the materials (Figure 3b). Both HVL and TVL for the materials studied were determined to be inversely related to the linear attenuation coefficient (LAC) of each respective material. Overall, the identified HVL and TVL for the various materials examined show a mixed response to the shielding of ionizing radiation, particularly photons. Furthermore, as the thickness increases, the materials' capacity to attenuate high-energy photons also rises. This suggests that these materials can effectively reduce exposure to any photon-emitting radionuclides when used for indoor building finishes.

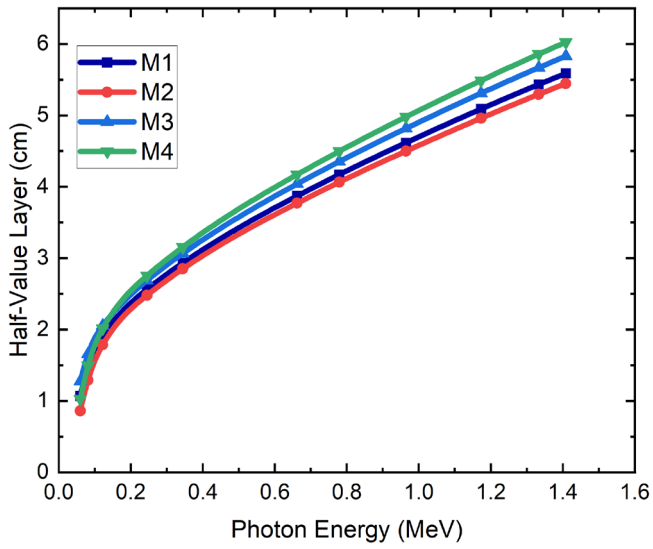

(a)

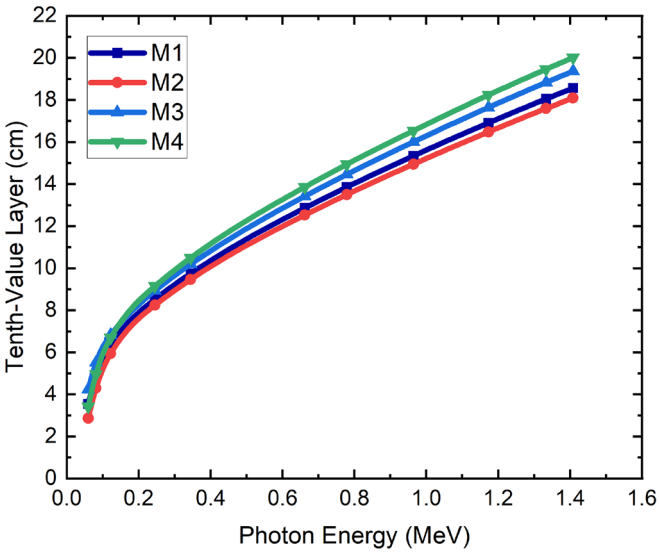

(b)

Fig. 3. (a) Half- (b) Tenth-Value Layer of the building materials as a function of photon energy.

Figure 4 illustrates the results related to the variation of mean free path (MFP) with photon energies for the selected building materials. The dependence of MFP on photon energy mirrors the trends seen in the HVL and TVL. The MFP values are lower at lower photon energies, while they increase as photon energy rises [39]. In addition, density directly affects the HVL and MFP value of a material. The higher the density, the better the compactness of the materials and the stronger its radiation shielding ability. The greater the density of a material,

the smaller the MFP, which indicates that high density materials have better radiation shielding performance when a high-energy photon pass through the materials of equal thickness. Based on these findings, it can be concluded that M2>M1>M3>M4, as materials with lower parameter values are deemed excellent absorbers of gamma rays [23,24,42].

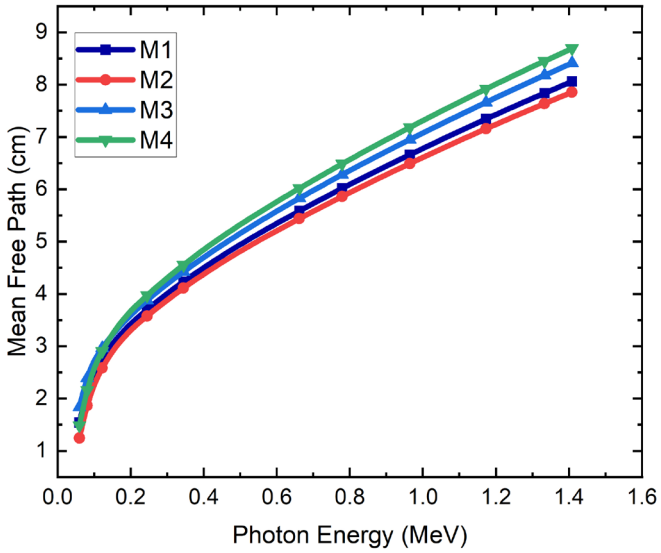

Fig. 4. Mean Free Path of the building materials as a function of photon energy.

Density and effective atomic number are two key factors that significantly impact the absorption and scattering of photons in materials [43]. Materials with a higher effective atomic number can more effectively diminish gamma-ray intensity due to having a larger number of electrons per atom [19,43,44]. Figure 5a illustrates the effective atomic number (Z_{eff}) of the materials examined at the photon energy relevant to this research. The figure indicates that the Z_{eff} for M4 (ceramic tiles) surpasses that of the other materials, while M2 (gypsum) exhibits the lowest Z_{eff} value. This higher Z_{eff} value for M4 is linked to the high atomic numbers of the elements (O, Mg, Al, Si, K, Ca, Fe) constituting this material compare to other materials especially concrete (M1) and gypsum (M2) that both has H content, a low atomic number element.

It was noted that as the photon energy approaches 0.3 MeV, the Z_{eff} values for all materials remain relatively stable. Figures 5 b – e depicts the behaviours of the studied building materials when subjected to various types of charged particulate radiations. Therefore, while M2 showed a low Z_{eff} value when interacting with photons, its interactions with alpha particles, electrons, protons, and carbon ions revealed that M2 performed better with the highest Z_{eff} value, whereas M3 (glass) displayed the lowest. This suggests that using these materials in construction beyond residential purposes could be advantageous in facilities dealing with radiation to minimize exposure and effectively attenuate radiation through a single material, compounds, or mixtures of elements.

The effective atomic number (Z_{eff}) is significant radiation shieling parameter as it provides a measure of how radiation interacts with a material, by indicating how readily a material absorbs radiations based on its composition [45]. Material with high Z_{eff} signifies its increase ability to interact with radiations, meaning that the material will absorb more radiation, making it useful as radiation shielding materials. Thus, materials with a high Z_{eff} have a greater probability of interacting with incoming radiation most especially photons through processes like photoelectric effect and Compton scattering leading to better absorption. Hence, while most of the highly penetrative radiation inside a building emanate from the terrestrial radionuclides from the rocks and soil upon which a building is erected. Figure 5a revealed that the applications of ceramic tiles in flooring of the building as interior decoration are sufficient enough compared to concrete flooring to attenuate the photons emitted by the natural occurring radionuclides of the terrestrial sources. In addition, this result further encourages the continuous lining of the walls of some section of the buildings such as the toilet/bathroom, kitchen and others with ceramic tiles. Figures 5b – e shows categorically that for charged particulate radiations that are less penetrating as photons (X- and gamma-rays), the use of gypsum as building ceilings, concrete as walls and glass as windows are justified to attenuate the particulate radiations external to the building.

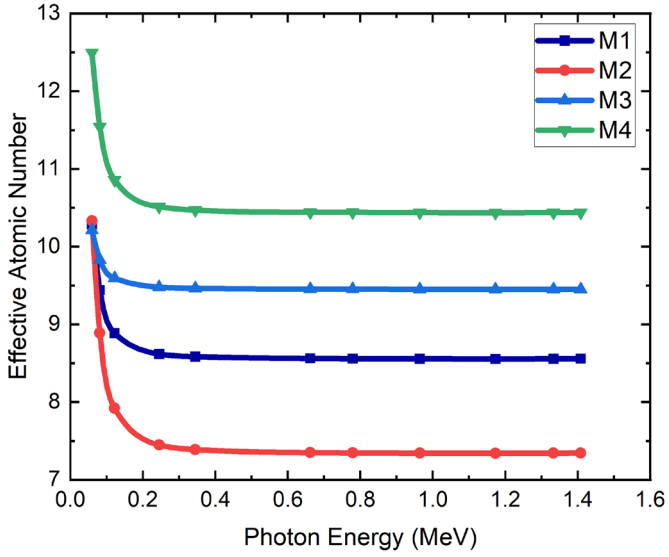

(a)

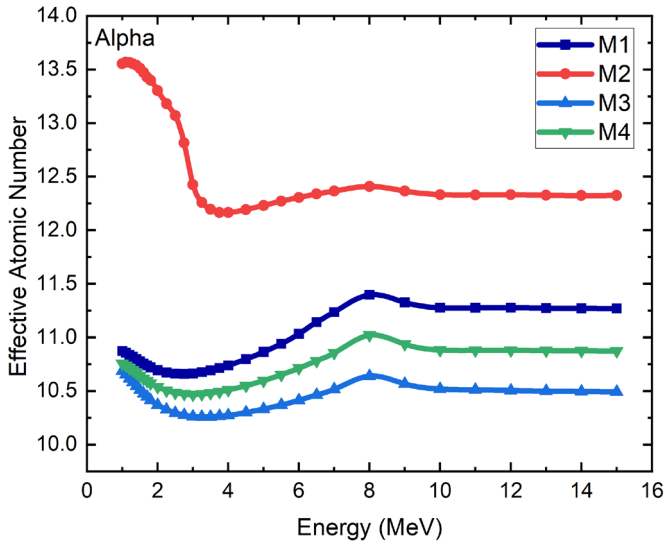

(b)

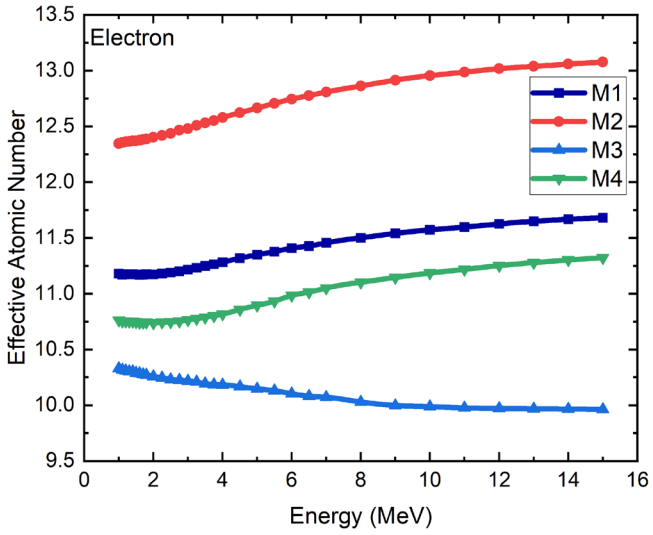

(c)

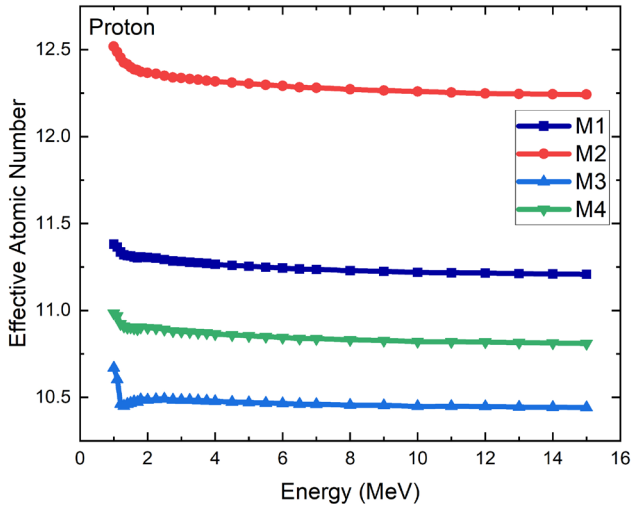

(d)

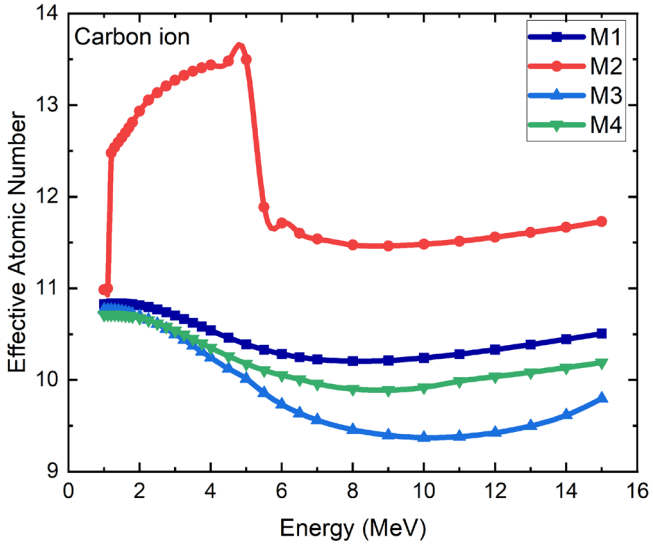

(e)

Fig. 5. Effective atomic number of the building materials for different radiation (a) photon (b) alpha (c) electron (d) proton (e) carbon ion.

However, the dynamic observed for the Z_{eff} for photon in Figure 5a changes as seen in Figure 6, which illustrates the variation of effective electron density (N_{eff}) concerning photon energy. The N_{eff} of a material is a crucial factor in radiation shielding because it directly determines how effectively a material can absorb and attenuate radiation, most especially photons. The higher the N_{eff}, the more interactions occur with the radiation, leading to better shielding capabilities. Hence, Figure 6 further collaborate all previous discussion that gypsum (M2) performs better compare to other materials investigated.

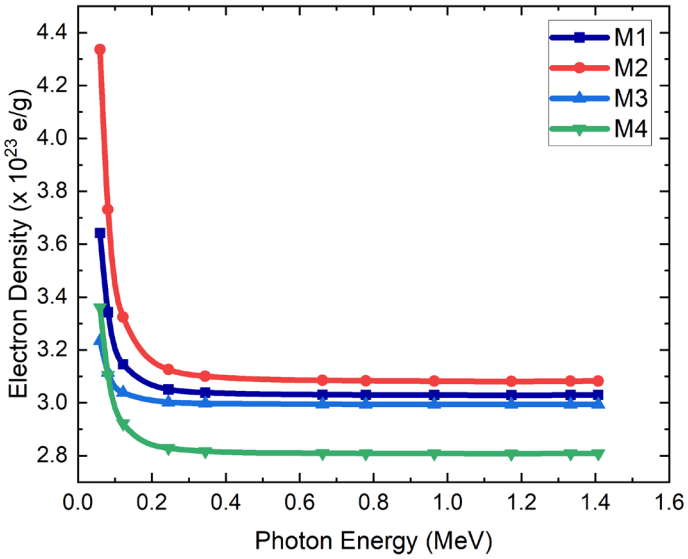

Fig. 6. Electron density of the building materials as a function of photon energy.

Displayed in Figure 7 are the equivalent atomic numbers (Z_{eq}) for each of the building materials examined in this study. These values were utilized to interpolate the GP fitting parameters for all the materials under investigation. For instance, the Z_{eq} and GP fitting parameters for M1 (concrete) are presented in Table 2. The EBF of a specific material ranged from 0.015 to 15 MeV as a function of photon energy.

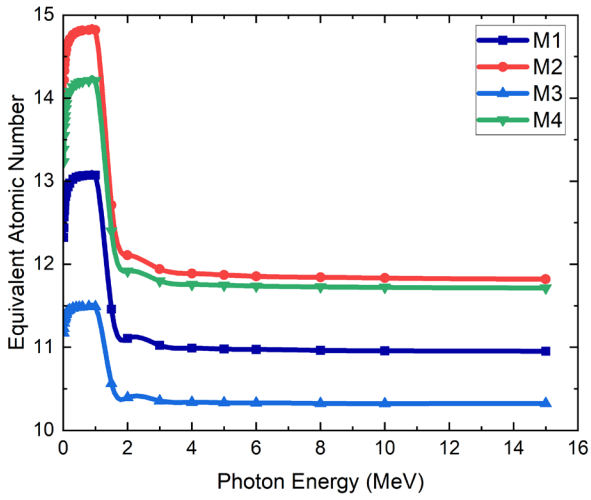

Fig. 7. Equivalent atomic number variation with different energy of photons for the investigated materials.

Table 2. The Z_{eq} and GP fitting parameters for M1 (Concrete) in the range 0.015 – 15 MeV.

Energy (MeV)	Z_{eq}	a	b	c	d	X_k
0.015	12.32	0.209	1.034	0.399	-0.135	14.055
0.02	12.44	0.197	1.077	0.414	-0.104	14.102
0.03	12.57	0.194	1.250	0.433	-0.103	14.797
0.04	12.65	0.158	1.527	0.521	-0.085	14.913
0.05	12.71	0.106	1.860	0.657	-0.054	15.719
0.06	12.75	0.096	2.256	0.720	-0.058	13.382
0.08	12.82	0.030	2.695	0.944	-0.032	13.116
0.1	12.86	-0.012	2.881	1.126	-0.017	12.888
0.15	12.93	-0.059	2.887	1.363	0.008	21.294
0.2	12.98	-0.074	2.764	1.457	0.012	16.996
0.3	13.02	-0.085	2.544	1.509	0.017	16.237
0.4	13.05	-0.085	2.401	1.497	0.019	16.419
0.5	13.06	-0.083	2.285	1.473	0.019	16.403
0.6	13.07	-0.081	2.196	1.446	0.023	17.143
0.8	13.07	-0.072	2.078	1.384	0.020	16.169
1	13.07	-0.066	1.993	1.335	0.021	15.847
1.5	11.46	-0.049	1.873	1.234	0.017	14.885
2	11.11	-0.034	1.794	1.154	0.012	14.617
3	11.02	-0.011	1.684	1.056	0.001	10.622
4	10.99	0.006	1.606	0.992	-0.009	12.882
5	10.98	0.016	1.536	0.956	-0.020	15.195
6	10.98	0.031	1.494	0.914	-0.025	11.410
8	10.96	0.033	1.406	0.902	-0.026	13.517
10	10.96	0.043	1.347	0.876	-0.033	13.200
15	10.95	0.064	1.263	0.823	-0.056	14.359

Furthermore, Figure 8 depicts the exposure buildup factor (EBF) of the samples at a constant penetration depth. The EBF values exhibited a marked increase from 0 to 2 MeV followed by a significant decline thereafter. It was also noted that as the MFP increased, the EBF value appeared considerably larger. This observation can be attributed to the Compton scattering process at this energy level. In this region, gamma ray photons are not entirely extracted, yet their energies diminish. These photons were present within the sample for extended periods, resulting in multiple Compton scattering interactions, which elevated the EBF to a higher value. The EBF results across all the materials analysed showed roughly similar values between 2 and 15 MeV, suggesting that EBF was not influenced by the composition of the materials in this segment. The EBF trend observed between 2 and 15 MeV was a result of the pair production process, which is a significant photon interaction phenomenon at these elevated energies. Moreover, among the materials studied, M3 exhibited the highest EBF value while M2 displayed the lowest. The diminutive EBF values for M2 may be linked to the material's higher Z_{eq} (Figure 7). Additionally, Figure 8 reveals that the EBF value of the material increased with greater penetration depth. The lowest EBF value for all samples was recorded at 1 MFP (Figure 8a), whereas the highest value was noted at 40 MFP (Figure 8d). This finding can be attributed to multiple dispersions occurring at a greater penetration depth.

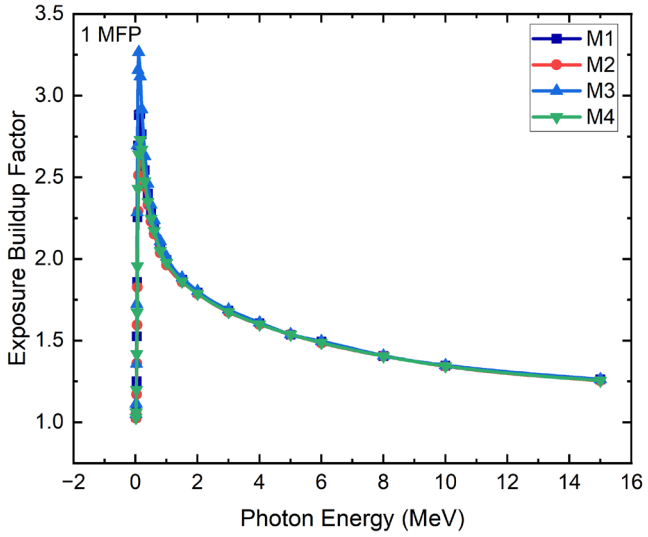

(a)

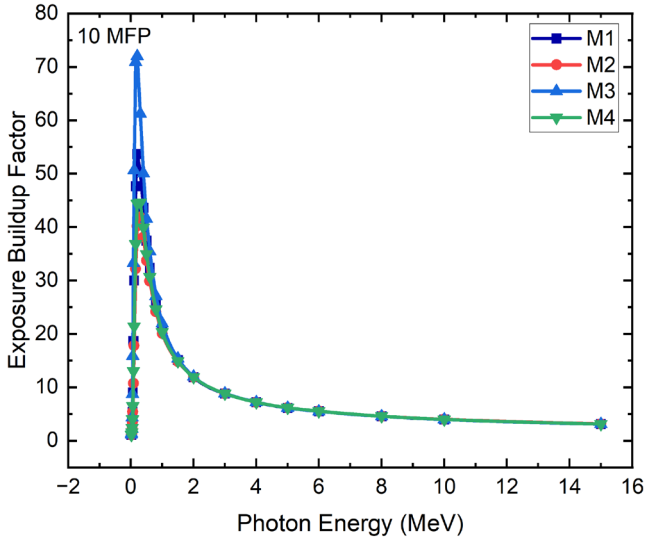

(b)

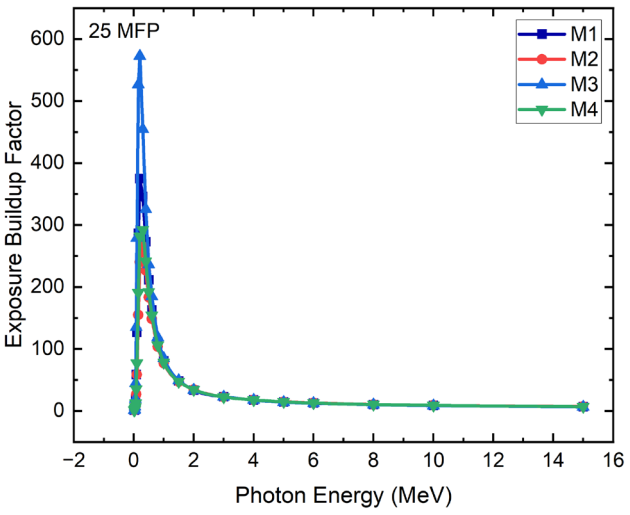

(c)

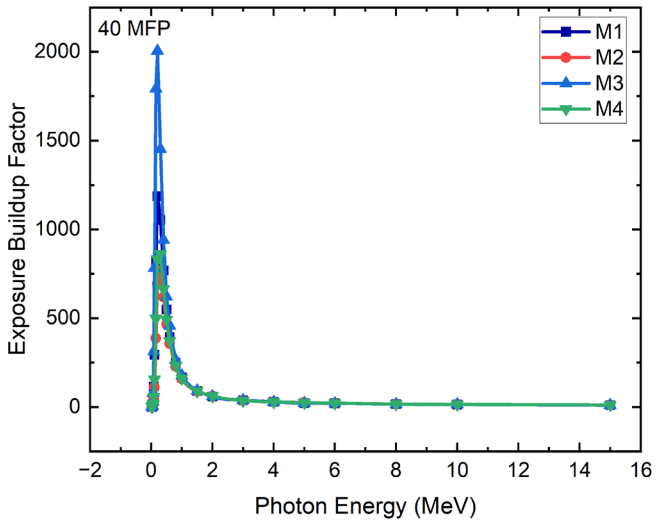

(d)

Fig. 8. The variation of EBF with -ray energy for the investigated polymers at (a) 1 (b) 10 (c) 25 and (d) 40 MFP

Figure 9 illustrates how the EBF varies with penetration depth at specific constant energies of 0.015, 0.15, 1.5, and 15 MeV respectively. In the low-energy range (9a), the EBF displayed a consistent increase characterized by a sigmoid pattern; at 0.15 MeV (9b), the EBF rose following an exponential trend with considerable fluctuations in EBF values. In both instances, material M3 exhibited the greatest growth, while M2 showed the least increase. Furthermore, in the low-energy ranges of 0.015 MeV and 0.15 MeV, it was noted that materials with lower Z_{eq} (M3 and M1) exhibited higher EBF values, in contrast to materials with higher Z_{eq} (M2 and M4), which had lower EBF values. Therefore, it can be concluded that the EBF values are influenced by the chemical composition in the low-energy regions (0.015 MeV and 0.15 MeV).

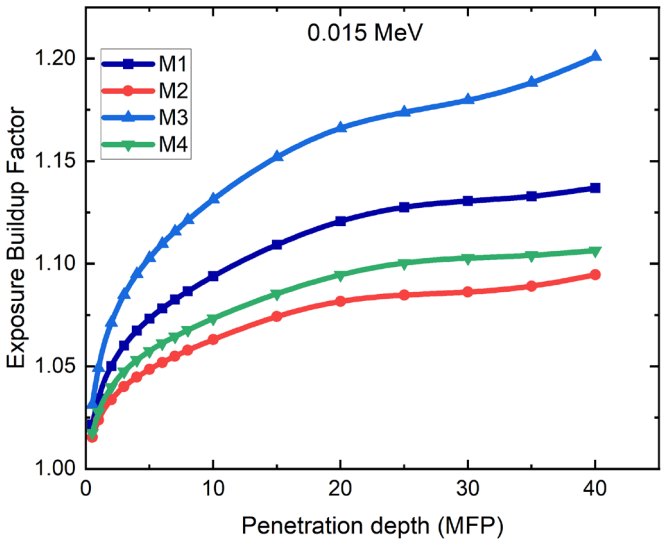

(a)

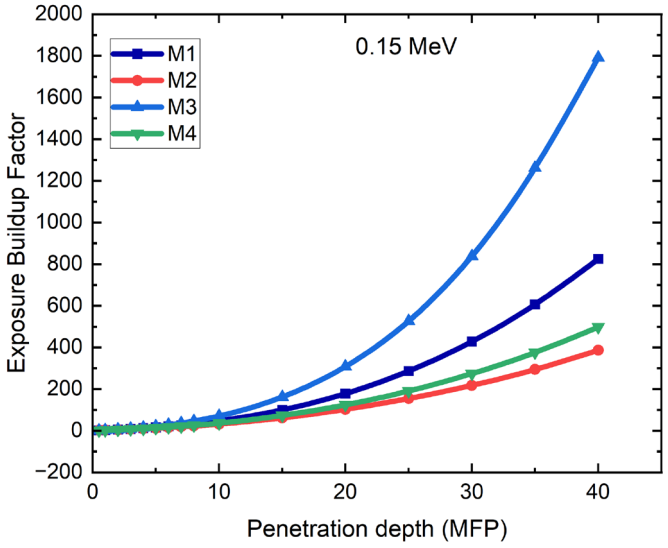

(b)

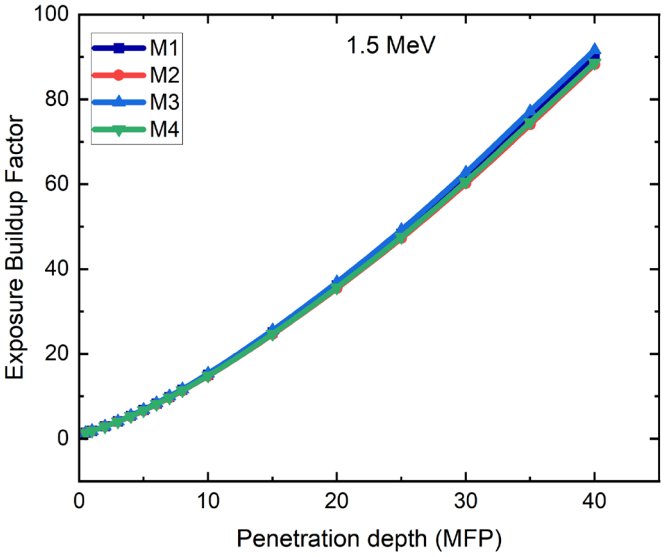

(c)

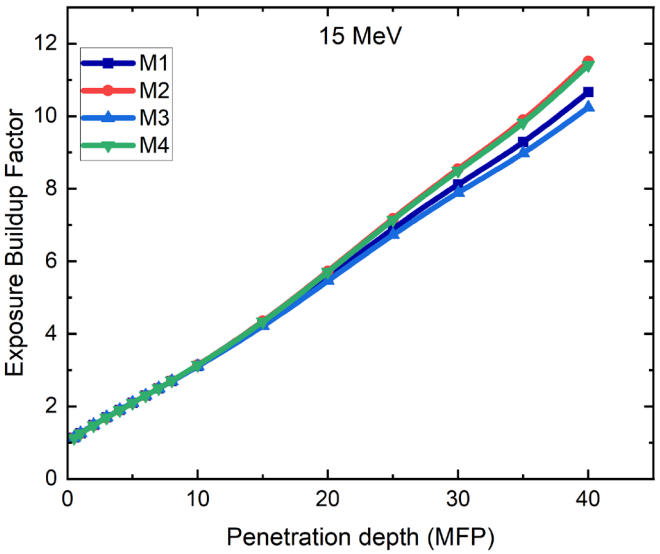

(d)

Fig. 9. Variation of exposure buildup factors with penetration depth (MFP) at (a) 0.015, (b) 0.15, (c) 1.5 and (d) 15 MeV.

At low incident photon energies, the Beer-Lambert law experiences minimal violation, even with a large penetration depth of 40 MFP [46]. This indicates that the photoelectric effect predominates in the lower energy regions while the likelihood of Compton scattering is almost insignificant. With a fixed incident photon energy of 1.5 MeV (Figure 9c), the growth pattern of EBF mirrors that observed at 0.15 MeV, with values becoming almost independent of the chemical composition (Z_{eq}). Although the magnitude of the EBF has decreased, the frequency of Compton scattering events has increased, making it difficult to identify the interacting material. At very high incident photon energy (Figure 9d) and for penetration depths exceeding 15 MFP, M2 and M4 (with maximum Z_{eq}) exhibit the highest EBF values, while M3 (with minimum Z_{eq}) shows the lowest EBF values. This change in trend can be attributed to the fact that at this incident photon energy (15 MeV), pair production becomes the primary interaction process for photons. Overall, it was noted that EBF tends to rise as the penetration depth increases.

Hence, while ionizing radiation is considered hazardous to human health even for indoor radiation exposure, it can be emphatically stated based on the findings of the present study that the applications of these materials (concrete, gypsum, glass and ceramic tiles) for interior building decoration purposes are justified, as they are sufficient in shielding against indoor radiations. Thus, their role in residential buildings should not be limited to just structural design and aesthetic appeal but rather be extended to radiation shielding. The materials can also be applied in building structures whose activities are not radiation intensive such as industries, research institute and several others. In addition, the attributes of these materials can be enhanced by coating with high atomic number material such as lead, steel or iron for radiation intensive activities like nuclear research facilities and hospitals.

4.1 Limitations of the study

Although, this study applied theoretical based computational method using Phy-X/PSD software, a very robust tool developed for calculating parameters relevant to radiation shielding and dosimetry, however, some limitations must be acknowledged. The accuracy in calculating the shielding parameters is heavily reliant on the exact definition of the material composition and its density as well as selection of appropriate energy range or radionuclides. Failure to do this, may introduce errors, thereby underestimating or overestimating result of each parameter. To address this limitation, future studies could explore the experimental confirmation the radiation shielding effectiveness of the building materials at the energy range of the radionuclides investigated in this study.

5. CONCLUSION

The radiation shielding characteristics, including photon mass and linear attenuation coefficients, half- and tenth-value layers, mean free path, effective atomic number, and exposure buildup factor of four different building materials were examined computationally for their effectiveness in radiation shielding. The results revealed that gypsum (M2) performs better compared to concrete (M1), glass (M3), and ceramic tiles (M4). This suggests that gypsum is more effective at attenuating gamma rays. This phenomenon can be linked to the slight variations in the density of the materials studied. This study furthermore, encourage the continuous usage of ceramic tiles in building flooring compared to concrete flooring, as ceramic tiles proofed to be sufficient in attenuating penetrative radiations from gamma-emitting radionuclides of rocks and soil more than concrete. This also applies to lining of the walls of buildings with ceramic tiles. For charged particulate radiations that are less penetrating and whose energy are low, the usage of gypsum as building ceilings, concrete as walls and glass as windows are justified to attenuate the particulate radiations. In addition, the exposure buildup factor for the examined materials increased with depth of penetration, being highest for 40 MFP and lowest for 1 MFP. This study concludes that the studied building materials can be used independently for low-energy applications or in conjunction with other high-Z materials for high-energy gamma-ray shielding. As a result, while significant attention is given to creating aesthetically pleasing interior designs, end users remain safe from a radiological perspective, as these materials effectively shield against penetrating radiation. The study also recommends experimental confirmation of the radiation shielding effectiveness of the assayed building materials at the same energy range of investigated radionuclides, as well as other building materials not captured by the study.

REFERENCES

[1] M. J. Egenhofer. Geographic Information Science: Second International Conference, GIScience 2002, Boulder, CO, USA, September 25–28, 2002. Proceedings. Springer Science & Business Media. 2002, p. 110. doi: https://doi.org/10.1007/3-540-45799-2

[2] S. Yesmin, B. S. Barua, M. U. Khandaker, M. T. Chowdhury, M. Kamal, M.A. Rashid, M.M.H. Miah and D.A. Bradley,"Investigation of ionizing radiation shielding effectiveness of decorative building materials used in Bangladeshi dwellings, Radiation Physics and Chemistry. doi: http://dx.doi.org/10.1016/j.radphyschem.2016.11.017

[3] M. K. Lawal, P. S. Ayanlola, O. O. Oladapo, O. M. Oni, and A. A. Aremu, "Assessment of radon exhalation rates in mineral rocks used in building decoration in Nigeria". Radiation Protection Environment; 2021, 44(3); 161 – 166. doi: http://dx.doi.org/10.4103/rpe.rpe_39_21

[4] A. A. Aremu, O. M. Oni, O. O. Oladapo, E. A. Oni, P. S. Ayanlola, and M. K. Lawal, "Determination of Radon Exhalation Rate from different Mixtures of Concrete" Materials Today: Proceedings, 2023, 86: 47 – 50. doi: https://doi.org/10.1016/j.matpr.2023.02.224

[5] G. A. Isola, P. S. Ayanlola, O. I. Ayantunji, and O. P. Bayode, "Comparative Study on the Contribution of Asbestos and Gypsum Building Materials to Environmental Radioactivity and Its Radiological Implication" International Journal of Sciences: Basic and Applied Research; 2021 56(2); 263 - 271 https://www.gssrr.org/index.php/JournalOfBasicAndApplied/article/view/12379/5971

[6] United Nations Scientific Committee on the effects of Atomic Radiation (UNSCEAR) 2000. Report of UNSCEAR to the general assembly, United Nations, New York, USA

[7] ICRP The 2007 Recommendations of the International Commission on Radiological Protection. ICRP Publication 103. Annals of the ICRP, 2007, 37(2-4).

[8] J. H. White. Your Complete Guide: Materials That Block Radiation. https://radetco.com/your-complete-guide-materials-that-block-radiation/ 2024

[9] I. C. P. Salinas, C. C. Conti and R. T. Lopes. "Effective density and mass attenuation coefficient for building material in Brazil". Appl Radiat Isot 2006; 64: 8–13. doi: http://dx.doi.org/10.1016/j.apradiso.200 5.07.003

[10] I Akkurt and H. Akyıldırım. "Radiation transmission of concrete including pumice for 662, 1173 and 1332 keV gamma rays". Nucl Eng Des 2012; 252: 163–166. doi: https://doi.org/10.1016/j.nucengdes.2012.07.008

[11] S. Yasmin, B. S. Barua, M. U. Khandaker, F. U. Z. Chowdhury, M. A. Rashid, D. A. Bradley, M. A. Olatunji and M. Kamal. "Studies of ionizing radiation shielding effectiveness of silica-based commercial glasses used

in Bangladeshi dwellings". Results Phys 2018a; 9: 541–549. doi: https://doi.org/10.1016/j.rinp.2018.02.075

[12] S Yasmin, Z. S. Rozaila, M. U. Khandaker, B. S. Barua, F. U. Z. Chowdhury, M. A. Rashid and D. A. Bradley. "The radiation shielding offered by the commercial glass installed in Bangladeshi dwellings". Rad Effects Defects Solids 2018b; 173: 657–672. doi: https://doi.org/10.1080/10420150.2018.1493481

[13] U. Cevik, N. Damla, R. Van Grieken and M. Vefa Akpınar. "Chemical composition of building materials used in Turkey". Constr Build Mater 2011; 25: 1546–1552. doi: https://doi.org/10.1016/j.conbuildmat.2010.08.011

[14] H. Binici, O. Aksogan, A. H. Sevinc and A. Kucukonder. "Mechanical and radioactivity shielding performances of mortars made with colemanite, barite, ground basaltic pumice and ground blast furnace slag". Constr Build Mater 2014; 50: 177–183. doi: https://doi.org/10.1016/j.conbuildmat.2013.09.033

[15] G. Tyagi, A. Singhal, S. Routroy, D. Bhunia, and M. Lahoti. "A review on sustainable utilization of industrial wastes in radiation shielding concrete". Mater Today: Proc. 2020;32:746–51. doi: https://doi.org/10.1016/j.matpr.2020.03.474

[16] P. Tamayo, C. Thomas, J. Rico, S. Pérez, and A. Mañanes. "Radiation shielding properties of siderurgical aggregate concrete". Construct Build Mater. 2022; 319:126098. doi: https://doi.org/10.1016/j.conbuildmat.2021.126098

[17] S. Barbhuiya, B. B. Das, P. Norman, and T. Qureshi. "A comprehensive review of radiation shielding concrete: Properties, design, evaluation, and applications" Structural Concrete. 2024; 1–47. doi: https://doi.org/10.1002/suco.202400519

[18] I. Akkurt, H. Akyıldırım, B. Mavi, S. Kilincarslan and C. Basyigit. "Radiation shielding of concrete containing zeolite". Rad Meas 2010; 45: 827–830. doi: https://doi.org/10.1016/j.radmeas.2010.04.012

[19] S. Yasmin, M. U. Khandaker, B. S. Barua, M. N. Mustafa, F. U. Z. Chowdhury, M. A. Rashid and D. A. Bradley. "Ionizing radiation shielding effectiveness of decorative building materials (porcelain and ceramic tiles) used in Bangladeshi dwellings". Indoor and Built Environment 2018. doi: https://doi.org/10.1177/1 420326X18798883

[20] A. Santhanam. "What makes glass a class apart" (2024, May 28) https://wfmmedia.com/the-use-of-glass-in-building-design-blending-exteriors-with-interiors/

[21] K. Hellstrom, A. Dioszegi, and L. Diaconu. "A broad literature review of density measurements of liquid cast iron. Metals". 2017 doi: https://doi.org/10.3390/met7050165

[22] D.F. Jackson, and D.J. Hawkes. "X-ray attenuation coefficients of elements and mixtures", Phys. Rep. 70 (3) (1981) 169–233 doi: https://doi.org/10.1016/0370-1573

[23] M. T. Alabsy, J. S. Alzahrani, M. I. Sayyed; M. I. Abbas, D. I. Tishkevich, A. M. El-Khatib, M. Elsafi "Gamma-Ray Attenuation and Exposure Buildup Factor of Novel Polymers in Shielding Using Geant4 Simulation" Materials 2021, 14, 5051. doi: https://doi.org/10.3390/ma14 175051

[24] Q. Chang, S. Guo, and X. Zhang. "Radiation shielding polymer composites: Ray-interaction mechanism, structural design, manufacture and biomedical applications". Materials and Design 233(2023) 112253. doi: https://doi.org/10.1016/j.matdes.2023.112253

[25] B. Mavi. "Experimental investigation of γ-ray attenuation coefficients for granites", Ann. Nucl. Energy 44 (2012) 22–25. doi: https://doi.org/10.1016/j. anucene.2012.01.009

[26] C. More, P. Pawar, M. Badawi, and A. Thabet. "Extensive theoretical study of gamma-ray shielding parameters using epoxy resin-metal chloride mixtures", Nucl . Technol. Radiat. Prot. 35 (2) (2020) 138–149. doi: http://dx.doi.org/10.2298/NTRP2002138M

[27] K.A. Matori, M.I. Sayyed, H.A.A. Sidek, M.H.M. Zaid, and V.P. Singh, "Comprehensive study on physical, elastic and shielding properties of lead zinc phosphate glasses", J. Non Cryst. Solids 457 (2017) 97–103. doi: https://doi.org/10.1016/j. jnoncrysol.2016.11.029

[28] M. Mariyappan, K. Marimuthu. M. I. Sayyed, M. G. Dong, and U. Kara. "Effect Bi2O3 on the physical, structural and radiation shielding properties of Er3+ ions doped bismuth sodiumfluoroborate glasses". J. Non-Cryst. Solids 2018, 499, 75–85. doi: https://doi.org/10.1016/j.jnoncrysol.2018.07.025

[29] Y. S. Rammah, A. A. Ali, R. El-Mallawany, and F. I. El-Agawany. "Fabrication, physical, optical characteristics and gamma-ray competence of novel bismo-borate glasses doped with Yb2O3 rare earth". Phys. B Condens. Matter. 2020, 583, 412055. doi: https://doi.org/10.1016/j.physb.2020.412055

[30] M. Elsafi, M. A. El-Nahal, M. F., Alrashedi, O. I. Olarinoye, M. I. Sayyed, M. U. Khandaker, H. Osman, S. Alamri, and M. I. Abbas. Shielding Properties of Some Marble Types: A Comprehensive Study of Experimental and XCOM Results. Materials 2021, 14, 4194. doi: https://doi.org/10.3390/ma14154194

[31] E. Şakar, O. F. Özpolat, B. Alım., M. I. Sayyed, and M. Kurudirek. "Phy-X / PSD: Development of a user-friendly online software for calculation of parameters relevant to radiation shielding and dosimetry", Radiation Physics and Chemistry 2019, doi: https://doi.org/10.1016/j.radphyschem.2019.108496

[32] L. Gerward, N. Guilbert, K. B. Jensen, and H. Levring. "X-ray absorption in matter. Reengineering XCOM". Radiat Phys Chem. 2001 60, 23-24. doi: https://doi.org/10.1016/S0969-806X(00)00324-8

[33] L. Gerward, N. Guilbert, K. B. Jensen, and H. Levring. "WinXCom - a program for calculating X-ray attenuation coefficients". Radiat Phys Chem 2004, 71, 653-654. doi: https://ui.adsabs.harvard.edu/link_gateway/2004RaPC...71..653G/doi:10.1016/j.radphyschem.2004.04.040

[34] M. J. Berger, J. H. Hubbel, S. M. Seltzer, J. Chang, J. S. Coursey, R. Sukumar, D. S. Zucker, and K. Olsen. "XCOM: photon cross section database (version 1.5). National Institute of Standards and Technology, Gaithersburg [internet]. 2010 [cited 2024 Aug. 14]. Available from: https://physics.nist.gov/PhysRefData/Xcom/html/xcom1.html

[35] R. Nowotny. "XMuDat: Photon attenuation data on PC". IAEA Report IAEA-NDS 195, 1998.

[36] Z. Yalcin, O. Icelli, M. Okutan, R. Boncukcuoglu, O. Artun, and S. Orak. "A different perspective to the effective atomic number (Z(eff)) for some boron compounds and trommel sieve waste (TSW) with a new computer program ZXCOM". Nucl Instrum Meth A 2012, 686, 43-47. doi: https://doi.org/10.1016/j.nima.2012.05.041

[37] O. Eyecioğlu, A. El-Khayatt, Y. Karabul, M. Çağlar, O. Toker, and O. Đçelli. "BXCOM: a software for computation of radiation sensing". Radiation Effects and Defects in Solids 2019. 174, 506-518. doi: https://doi.org/10.1080/10420150.2019.1606811

[38] N. A. M. Rusni, H. Laoding, and A. Amat "Theoretical Ionizing Radiation Shielding Parameters of Thulium Doped Zinc Borotellurite Glass" E3S Web of Conferences 481, 03009 (2024). doi: https://doi.org/10.1051/e3sconf/202448103009

[39] S. I. Mohammed, and A. H. Taqi "Mass attenuation coefficient of electromagnetic radiation for human tissues" Journal of Radiation Research and Applied Sciences 18 (2025) 101255. doi: https://doi.org/10.1016/j.jrras.2024.101255

[40] E. S. A. Waly, M. A. Fusco and M. A. Bourham. "Gamma-ray mass attenuation coefficient and half value layer factor of some oxide glass shielding materials". Ann Nucl Energy 2016; 96: 26–30. doi: https://doi.org/10.1016/j.anucene.2016.05.028

[41] M. I. Abbas, A. M. El-Khatib, M. Elsafi, S. N. El-Shimy, M. F. Dib, H. M. Abdellatif, R. Baharoon, and M. M. Gouda. "Investigation of Gamma-Ray Shielding Properties of Bismuth Oxide Nanoparticles with a Bentonite–Gypsum Matrix". Materials 2023, 16, 2056. doi: https://doi.org/10.3390/ma16052056

[42] M.R. Kaçal, F. Akman, M.I. Sayyed, and F. Akman. "Evaluation of gamma-ray and neutron attenuation properties of some polymers", Nucl. Eng. Technol. 51 (3) 2019 818–824, doi: https://doi.org/10.1016/j.net.2018.11.011.

[43] I. Akkurt. "Effective atomic and electron numbers of some steels at different energies". Ann Nucl Energy 2009; 36: 702–1705. doi: https://doi.org/10.1016/j.anucene.2009.09.005

[44] U. Cevik, and H. Baltas. "Measurement of the mass attenuation coefficients and electron densities for BiPbSrCaCuO superconductor at different energies". Nucl Instr Meth Phys Res B 2007; 256: 619–625. doi: https://doi.org/10.1016/j.nimb.2007.01.131

[45] M. Kurudirek "Effective atomic numbers of different types of materials for proton interaction in the energy region 1 keV–10 GeV". Nuclear Instruments and Methods in Physics Research Section B: Beam Interactions with Materials and Atoms, 336, 2014 130–134. doi: https://doi.org/10.1016/j.nimb.2014.07.008

[46] M. I. Sayyed, M. Y. AlZaatreh, K. A. Matori, H. A. A. Sidek, and M. H. M. Zaid. "Comprehensive study on estimation of gamma-ray exposure buildup factors for smart polymers as a potent application in nuclear industries", Results in Physics 2018. doi: https://doi.org/10.1016/j.rinp.2018.01.057